Functional Neuroimaging Data Characterisation Via Tensor Representations

Christos Chatzichristos*
National and Kapodistrian University of Athens
Department of Informatis and Telecommunications, Greece
chrichat@hotmail.com

Abstract

In this dissertation we aimed at investigating the possible gains from exploiting the 3-dimensional nature of the brain images, through a higher-order tensorization of the fMRI signal, and the use of less restrictive generative tensor models. In this context, the higher-order Block Term Decomposition (BTD) and the PARAFAC2 tensor models are considered, for first time in fMRI blind source separation. In order to test the proposed BSS methods and in order to understand the limitations and challenges that doctors face, a novel fMRI protocol was also designed and fMRI data from volunteers were collected. The last problem that this thesis touches upon is the fusion of fMRI and electroengephalography (EEG). Analyzing both EEG and fMRI measurements is highly beneficial for studying brain function because these modalities have complementary spatio-temporal resolutions

1 Introduction

Brain tasks involving action, perception, cognition, memory retrieval, etc., are performed via the simultaneous activation of a number of brain regions, which are engaged in proper interactions in order to effectively execute a specific task. In functional Magnetic Resonance Imaging (fMRI), brain activity is captured by detecting associated changes in blood flow within the brain [1]. In contrast, in Electroengephalography (EEG) the electrical activity, that is associated with the movement of charged atoms, which are emitted during a neural activation, is detected. Both EEG and fMRI measure ongoing neural activity during a certain period of time at specific locations at the surface of or inside the brain. The obtained data stream comprises a mixture of the source signals, which carry the useful information that is required by the neuroscientists in order to understand and "decipher" the various brain functions.

Extracting information from fMRI data commonly relies on simplifying assumptions and it is based on matrix-based approaches that fail to exploit the inherent multi-way structure of the brain data. In this PhD thesis, tensor (multi-way) models and associated algorithms are investigated that are adapted to the

*Dissertation Advisor: Sergios Theodoridis, Professor fMRI problem in order to assess their performance as compared to matrix-based schemes. Appropriate tensor factorizations are developed and studied. The key concept behind the methodologies presented in this thesis is to exploit the inherent structural information on different levels.

Since, in general, the processes underlying brain functions are not (yet) fully understood, it is of great significance to reduce any potential for biases and therefore minimize the assumptions imposed on the data. This motivates the use of Blind Source Separation (BSS) techniques [2]; the localization of the respective to each task activated areas in the human brain is a challenging BSS problem, in which the sources are a result of a combination of spatial maps (activated areas) and time-courses (timings of activation).

Furthermore, in order to understand a system as complex as the human brain, multimodal measurements can be beneficial, since they are able to capture complementary aspects of the same system. In the field of neuroimaging and brain mapping, the complementary nature of the (spatiotemporal) resolutions of the electroencephalography (EEG) and the functional Magnetic Resonance Imaging (fMRI) motivates for their fusion for a better localization of the brain activity, both in time and space [3].

In this thesis, the advantages of the use of higher order tensors in the BSS of fMRI are studied. The combination of EEG and fMRI is also explored in order to improve the results of BSS. Furthermore, a case study is developed and an fMRI protocol has been designed in order to test how the presence of semantic faces, emojis, affect the memory retrieval mechanism of the brain. In this context, all the methods that have been deployed in this thesis have been used in order to test their performance. A chapter-by-chapter abstract is given below.

2 Multilinear algebra

Tensors are arrays (of order higher than two), a generalization of matrices. Matrices are two-way arrays and can also be considered as second-order tensors; there are three- and higher-way arrays (or higher-order) tensors. Tensor algebra has many similarities but also significant and striking differences with matrix algebra.

The ith entry of a vector $\boldsymbol{a}$ is denoted a_i, while $a_{i,j}$ and $a_{i,j,k}$ denote an entry of a matrix $\boldsymbol{A} \in \mathbb{R}^{I\times J}$ and a tensor $\boldsymbol{\mathcal{A}} \in \mathbb{R}^{I\times J\times K}$, respectively. MATLAB notation is used for the rows or columns of a matrix or a tensor (e.g., $\mathbf{A}(i,:)$ is the ith row of matrx $\boldsymbol{A}$).

- The order of a tensor is the number of dimensions, also known as ways or modes.
- The mode–n unfolded (matricized) version $\boldsymbol{A}_{(n)} \in \mathbb{R}^{I_n\times I_1 I_s \cdots I_{n-1} I_{n+1} \cdots I_N}$ of an Nth-order tensor, $\boldsymbol{\mathcal{A}} \in \mathbb{R}^{I_1\times I_2\times\cdots\times I_N}$, results from mapping the tensor element $a_{(i_1,i_2,\ldots,i_N)}$ to a matrix element $a_{(i_n,j)}$
- $\boldsymbol{A}^\top$ and $\boldsymbol{A}^\dagger$ denote the transpose and the pseudo-inverse of a matrix $\boldsymbol{A}$.

The **Kronecker product** of two matrices $\boldsymbol{A} \in \mathbb{R}^{I\times J}$ and $\boldsymbol{B} \in \mathbb{R}^{K\times L}$ is denoted by the symbol $\otimes$ and the **Khatri-Rao product** (column-wise Kronecker) product of two matrices is denoted by $\odot$. Generally the **tensor rank $\boldsymbol{\mathcal{A}}$** is the minimal number of rank-1 tensors that yield $\boldsymbol{\mathcal{A}}$ in a linear combination and is usually denoted as R. Furthermore, the rank of the mode–n matricized version $\boldsymbol{A}_{(n)}$ of a tensor $\boldsymbol{\mathcal{A}}$ is known as **mode–n rank**. Generally the **multilinear rank** of a tensor is the N-tuplet of its N mode–n ranks [4].

3 Functional Magnetic Resonance Imaging

Functional Magnetic Resonance Imaging (fMRI) is a noninvasive technique for studying brain activity, which has been receiving an increasing attention in the last two decades or so. fMRI indirectly studies brain activity, by measuring fluctuations of the Blood Oxygenation Level Dependent (BOLD) signal [1]. BOLD fluctuation usually occurs between 3 to 10 seconds after the stimulus, and this effect is modeled by the so-called Haemodynamic Response Function (HRF). During an fMRI experiment and while the subject performs a set of tasks responding to external stimuli (task-related fMRI) or no tasks (resting-state fMRI), a series of 3-D brain images is acquired.

Increased neural activity requires more oxygen and glucose to be delivered. Hence, possible activation in an area of the brain results in a depletion of oxygen in the blood vessels near this area, which is followed by an influx of cerebral blood that overcompensates for the increase in demand, resulting in an excess of oxygenated blood in activated brain areas. The oxygen is transported through the blood vessels by means of hemoglobin molecules. Oxyhemoglobin (Hb) is diamagnetic, whereas deoxyhemoglobin (dHb) is a paramagnetic substance that produces microscopic magnetic field inhomogeneities which can be measured.

4 BSS for fMRI via higher-order tensor decompositions

The growing interest in neuroimaging technologies generates a massive amount of biomedical data that exhibit high dimensionality. Tensor-based analysis of brain imaging data has by now been recognized as an effective approach exploiting its inherent multi-way nature. In particular, the advantages of tensorial over matrix-based methods have previously been demonstrated in the context of functional magnetic resonance imaging (fMRI) source localization; the identification of the regions of the brain which are activated at specific time instances. However, such methods can also become ineffective in realistic challenging scenarios, involving, e.g., strong noise and/or significant overlap among the activated regions. Moreover, they commonly rely on the assumption of an underlying multilinear model generating the data. In the first part of this thesis, we aimed at investigating the possible gains from exploiting the 3-dimensional nature of the brain images, through a higher-order tensorization of the fMRI signal, and the use of less restrictive generative models.

Traditionally, after acquiring a 3-D fMRI image (with spatial dimensions $I_x \times I_y \times I_z$) at a time instance n (Fig. 1), the data (referred to as *folded* data) are reshaped to a lower dimension (*unfolded*), giving rise to a sequence of vectors, $\boldsymbol{t}_n$, for $n = 1, 2, \ldots, I_t$ (with $I_{xyz} = I_x \cdot I_y \cdot I_z$ voxels each). These I_t vectors (3-D images at different time instants) are stacked together to form

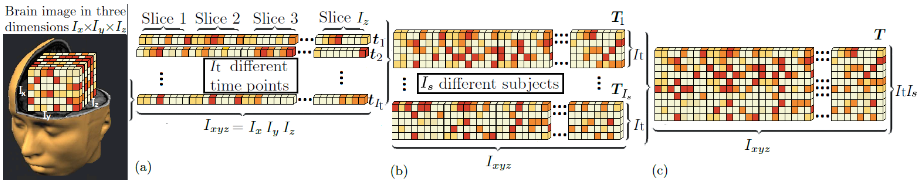

Figure 1: (a) Brain images unfolded in vectors and stacked in matrices (b) per subject and (c) for the multi-subject case.

a matrix (Fig. 1(a)). Such a matrix is formed for each one of the subjects, i.e., $\boldsymbol{T}_k, k = 1, 2, \ldots, I_s$ (I_s different subjects in the multi-subject case, Fig. 1(b)). These I_s matrices are in turn concatenated to form $\boldsymbol{T} \in \mathbb{R}^{I_t I_s \times I_{xyz}}$ (Fig. 1(c)), for which a decomposition is sought such that:

$$\boldsymbol{T} \approx \boldsymbol{M}\boldsymbol{A}^\top, \tag{1}$$

with $\boldsymbol{A} \in \mathbb{R}^{I_{xyz} \times R}$ containing the weights of the spatial maps and $\boldsymbol{M} \in \mathbb{R}^{I_t I_s \times R}$ containing the concatenated time-courses of all subjects, R being the estimated number of sources [5, 1]. Note that, in practice, the decomposition cannot be exact due to unmodeled phenomena including noise. In this way, the intrinsically 5th-order (dimension x $\times$ dimension y $\times$ dimension z $\times$ time $\times$ subjects) problem of a multi-subject fMRI analysis has been transformed into a 2nd-order one. This type of unfolding of higher-order data into two-way arrays leads to decompositions that are non-unique, unless specific assumptions on the involved factors are made. Moreover, and most importantly, such an unfolding can result in a loss of underlying informative correlations that may exist, because the neighborhood information is not respected. In this context, the approaches most frequently pursued are the Independent Component Analysis (ICA) [6], and Dictionary Learning [7]. ICA solves Eq. (1) by assuming that the matrix $\boldsymbol{A}$ contains statistically independent spatial maps in its columns, each one corresponding to a time-course in the associated column of the (mixing) matrix $\boldsymbol{M}$.

The multi-way nature of the data is preserved in multi-linear (tensor) models, which, in general, a) produce unique (modulo scaling and permutation ambiguities) representations under mild conditions, b) can improve the ability of extracting spatiotemporal modes of interest [5, 8, 9], and c) facilitate neurophysiologically meaningful interpretations [5]. The state-of-the-art in tensorial methods for analyzing multi-subject fMRI data include the Canonical Polyadic Decomposition (CPD)-based analysis [5] and the Tensor Probabilistic Independent Component Analysis (TPICA) [10].

Following the tensorial rationale, in contrast to the previously discussed unfolding, instead of forming a matrix $\boldsymbol{T}$ by concatenating the matrices $\boldsymbol{T}_{k=1,2,\ldots,I_s}$ (Fig. 1), the latter can be arranged to form a third-order tensor $\boldsymbol{\mathcal{T}} \in \mathbb{R}^{I_{xyz} \times I_t \times I_s}$ (Fig. 2). Hence, a tensor decomposition method can be mobilized for the BSS task instead of the matrix-based methods. Tensorial methods provide, in most of the cases, improved spatial and temporal localization of the activity, compared to the matrix-based approaches [5, 10].

CPD (or PARAFAC) [5] approximates a 3rd-order tensor (or an fMRI tensor in our case), $\boldsymbol{\mathcal{T}} \in \mathbb{R}^{I_{xyz} \times I_t \times I_s}$, by a sum of R (estimated number of sources)

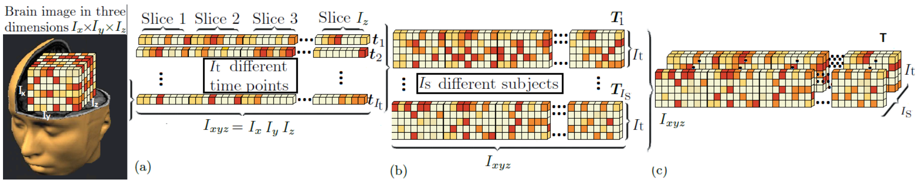

Figure 2: (a) Brain images unfolded in vectors and stacked in matrices (b) per subject and (c) in tensors in the multi-subject case.

rank-1 tensors (Fig. 4.a), namely

$$\boldsymbol{\mathcal{T}} \approx \sum_{r=1}^{R} \boldsymbol{a}_r \circ \boldsymbol{b}_r \circ \boldsymbol{c}_r. \tag{2}$$

The above can be equivalently written in the matricized form

$$\boldsymbol{T}_{(1)} \approx \boldsymbol{A}(\boldsymbol{C} \odot \boldsymbol{B})^\top, \tag{3}$$

and for the kth frontal slice of $\boldsymbol{\mathcal{T}}$ (analogous equations can be written for the horizontal and lateral slices):

$$\boldsymbol{T}_k \approx \boldsymbol{A}\boldsymbol{D}_k\boldsymbol{B}^\top, \quad k = 1, 2, \ldots, I_s, \tag{4}$$

where $\boldsymbol{A} = \left[\boldsymbol{a}_1, \boldsymbol{a}_2, \ldots, \boldsymbol{a}_R\right]$ is a matrix that contains the R spatial components (I_{xyz} voxels per component) and $\boldsymbol{B} = \left[\boldsymbol{b}_1, \boldsymbol{b}_2, \ldots, \boldsymbol{b}_R\right], \boldsymbol{C} = \left[\boldsymbol{c}_1, \boldsymbol{c}_2, \ldots, \boldsymbol{c}_R\right]$ are similarly defined matrices, which contain the associated time-courses (I_t time points) and the subject activation levels (I_s subjects), respectively. $\boldsymbol{D}_k$ is the diagonal matrix with the elements of the kth row of $\boldsymbol{C}$ on its diagonal. The main advantage of the CPD, besides its simplicity, is the fact that it is unique (up to permutation and scaling) under mild conditions.

The tensor formulation approach described inherit from the matrix-based counterparts the initial step of the unfolding of the 3-D spatial data into a *vector* $\boldsymbol{t}_n$. That is, they do not fully exploit the multi-way nature of the acquired data, which seems to be the natural path to follow for the task at hand.

In addition, the unfolding into vectors misses to fully reveal the low-rank content of the spatial signal, which can only be unveiled through a multi-way model. Furthermore, as it has been shown by Phan et al. [11], unfolding higher-order noisy data to lower-order tensors generally results in a loss of the accuracy in the respective decomposition.

A possible way to benefit from the findings mentioned above is to adopt an alternative type of data unfolding. For the unfolding proposed in this thesis, we adopt the mode-1 (frontal) matricization of the respective data tensor, $\boldsymbol{A}_n$ (Fig. 3(a)) (by symmetry, mode-2 or mode-3 can also be used with similar results). By stacking the I_t matrices together, a 3rd-order tensor, $\widetilde{\boldsymbol{\mathcal{T}}}_k$ (all the tensors generated by the suggested alternative unfolding will be denoted with a tilde), is formed for the kth subject (Fig. 3(c)). For I_s different subjects, a 4th-order tensor, $\widetilde{\boldsymbol{\mathcal{T}}}$, is created, by stacking together all 3-way tensors, $\widetilde{\boldsymbol{\mathcal{T}}}_k = \widetilde{\boldsymbol{\mathcal{T}}}(:, :, :, k)$. A 5th-order tensor (using directly the 3-D spatial brain images) could also be considered, albeit at a complexity increase.

Following those arguments, an alternative unfolding and a higher than 3rd-order tensor model is a more natural way to perform the unmixing of the sources.

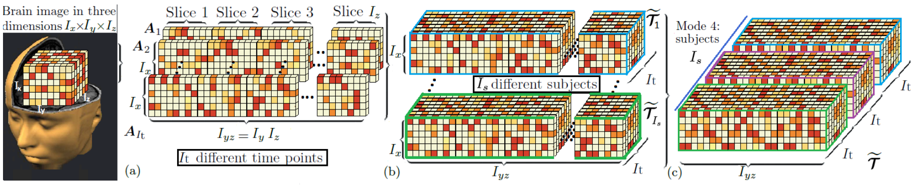

Figure 3: (a)Brain images unfolded in matrices and stacked in (b) 3rd-order tensors per subject and (c) 4th-order tensors for a number of subjects.

However, the use of CPD (and hence TPICA) with such a formulation can be problematic in cases where the components are not of rank one. As an alternative to CPD, the use of Block Term Decomposition (BTD) [4] in the 4-way (and 5-way) tensorization of the fMRI signal is investigated in this work, for the first time. The adoption of BTD (Fig.4.c) is dictated by the need of a more flexible model that reveals the low rankness of the spatial mode.

BTD is a generalization of CPD which can capture latent factors of rank higher than one in each component. In particular, the rank-$(L_r, L_r, 1, 1)$ BTD of the tensor $\widetilde{\mathcal{T}}_k \in \mathbb{R}^{I_x \times I_{yz} \times I_t}$ (Which is proposed) is given by:

$$\widetilde{\mathcal{T}} \approx \sum_{r=1}^{R} \boldsymbol{A}_r \circ \boldsymbol{b}_r \circ \boldsymbol{c}_r = \sum_{r=1}^{R} (\boldsymbol{X}_r \boldsymbol{Y}_r^\top) \circ \boldsymbol{b}_r \circ \boldsymbol{c}_r. \tag{5}$$

The two spatial factors are of low rank (L_r) while the time and subject factors are of rank one (those modes have not been folded and the assumption of rank one is still valid).

Furthermore, as mentioned previously one of the main assumption of the tensorial analysis of the BSS fMRI model (both with CPD and TPICA) is that the analyzed data are generated from a trilinear (or multilinear) model. This assumption, however, may prove to be quite strict in practice; for example, due to the natural intra-subject and inter-subject variability of the HRF. We will investigate the possible gains from the adoption of less strict models, such as PARAFAC2 (Fig.4.a).

PARAFAC2 [12] differs from CPD in that strict multilinearity is no longer a requirement. CPD assumes the *same* factors across *all* the different modes, whereas PARAFAC2 relaxes this constraint and allows variation across one mode (in terms of the values and/or the size of the corresponding factor matrix). It can be written in terms of the (here frontal) slices of the permuted tensor $\mathcal{T}^{(p)} \in \mathbb{R}^{I_t \times I_{xyz} \times I_s}$ as:

$$\boldsymbol{T}_k^{(p)} \approx \boldsymbol{B}_k \boldsymbol{D}_k \boldsymbol{A}^\top, \quad k = 1, 2, \dots, I_t, \tag{6}$$

and allowing $\boldsymbol{B}_k$ to be different for different k's.

In this context, the higher-order Block Term Decomposition (BTD) and the PARAFAC2 tensor models are considered, for first time in fMRI blind source separation. Furthermore it has been proposed an heuristic for the estimation of the inner rank L of the BTD decomposition for Blind Source Separation (BSS) of fMRI. The simulation results demonstrate the effectiveness of BTD for challenging scenarios (presence of noise, spatial overlap among activation regions) and the effectiveness of PARAFAC2 for scenarios where an inter-subject variability of the Haemodynamic Response Function (HRF) exists. Furthermore, a detailed analysis of a dataset which is openly available at the OpenfMRI database, has been performed.

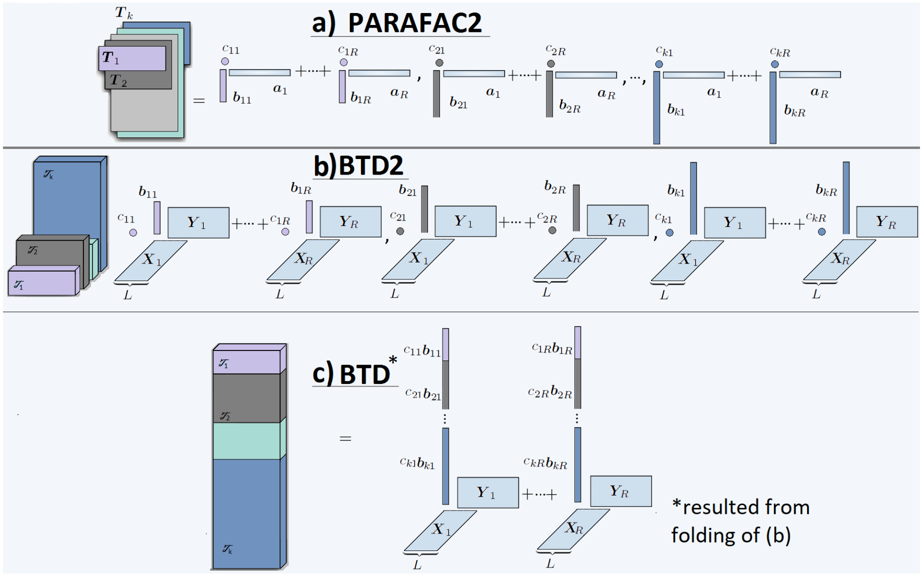

Figure 4: Non strictly multilinear tensor models: a) PARAFAC2 and b)BTD2. c) The more flexible model of BTD .

Aiming at combining the effectiveness of BTD in handling strong instances of noise and the potential of PARAFAC2 to cope with datasets that do not follow the strict multilinear assumption, we proposed a novel PARAFAC2-like extension of BTD, called BTD2 (Fig.4.b)

Using the (mode-1) unfoldings, $\widetilde{\boldsymbol{T}}^{(p)}_{k(1)}$, of the $\widetilde{\boldsymbol{\mathcal{T}}}^{(p)}_k = \widetilde{\boldsymbol{\mathcal{T}}}^{(p)}(:,:,:,k) \in \mathbb{R}^{I_t \times I_x \times I_{yz}}$ tensors (Fig. 2) yields the BTD2 decomposition:

$$\widetilde{\boldsymbol{T}}^{(p)}_{k(1)} = (\boldsymbol{B}_k \boldsymbol{S})\widetilde{\boldsymbol{D}}_k(\boldsymbol{X} \odot \boldsymbol{Y})^\top, k = 1, 2, \ldots, I_t. \tag{7}$$

The matrices $\boldsymbol{S} = \text{blockdiag}(\boldsymbol{1}_L^\top, \ldots, \boldsymbol{1}_L^\top)$ and $\widetilde{\boldsymbol{D}}_k = \text{blockdiag}(c_{k1}\boldsymbol{I}_L, \ldots, c_{kR}\boldsymbol{I}_L)$ appear in formulating BTD as CPD. Spatial matrices are defined as $\boldsymbol{X} = [\boldsymbol{X}_1, \boldsymbol{X}_2, \ldots, \boldsymbol{X}_R]$, $\boldsymbol{Y} = [\boldsymbol{Y}_1, \boldsymbol{Y}_2, \ldots, \boldsymbol{Y}_R]$ with $\boldsymbol{X}_i \in \mathbb{R}^{I_x \times L}$ and $\boldsymbol{Y}_i \in \mathbb{R}^{I_{yz} \times L}$. An Alternating Least Squares (ALS) algorithm is adopted for BTD2. The method was also tested using both synthetic and real data and we have exhibited that has superior performance in the presence of high noise, spatial overlap and difference in the HRFs among subjects.

5 How emojis influence memories derived from reading words

The second main part of this thesis, in addition to signal processing methods, also elaborates on practical aspects of fMRI. In order to test the proposed BSS methods and in order to understand the limitations and challenges that doctors face, as a part of a secondment in Bioiatriki SA, we designed a novel fMRI protocol and collected fMRI data from volunteers.We have tried to investigate the cognitive and behavioral effects of emojis in memory retrieval, in an effort to determine how emojis complement the written text. Communication plays an essential role in our everyday life and draws on both verbal (e.g., speech) and

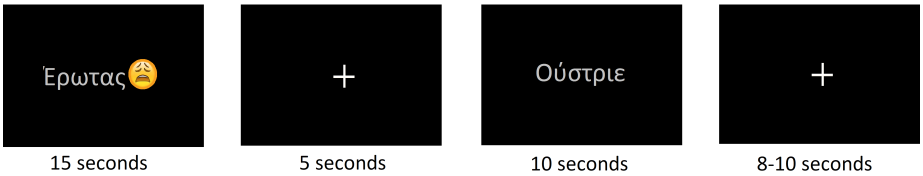

Figure 5: A block of the experimental task. A sentimental stimulus (Love and sad face) followed by a cross, a pseudoword and a second cross.

nonverbal (e.g., gestures, facial expressions, the tone of the voice) cues to convey information. Recently, the Computer-Mediated Communication (CMC), which lacks the subtle nonverbal cues, has become part of our life. The insertion of emoticons and emojis is one option to convey emotions in online text communication and compensate the lack of nonverbal communicative cues. Different stimuli were presented to the participants, which were composed of alternating positive and negative words combined with happy or sad emojis.

In this research we wanted to study the influence of emojis on memory retrieval from reading words of emotional content. Different volunteers were asked to rate 100 words based on their emotional content (happy or sad) as well as the ability to retrieve memories from those words (imageability). Eventually, using these results, two groups of 6 words were created, namely, those that exhibit the biggest difference in valance (most positive and most negative words) and simultaneously have similar mean values of arousal, imageability, and familiarity, to avoid secondary effects. The words selected were Love, Companionship, Hope, Life, Freedom and Truth for the group of happy words and Hospital, Melancholia, Pain, Sickness, Hopelessness and Abandonment for the group of sad words. With a similar way the most happy emoji was selected (Smiling face with open eyes) and the saddest one (weary face).

Different stimuli were presented to the participants. Those stimuli consisted of alternating words with happy or sad emotional content in combination with happy or sad emojis. Each word was combined once with the happy emoji and once with the sad emoji. Hence 24 different stimuli were created half of them with congruent semantic content (e.g. combination of a Happy word with the Happy emoji - HH) and the other with incongruent semantic content (e.g. combination of a Happy word with the Sad emoji - Hs). The total duration of the experiment was 15 to 17 minutes and consisted of 24 different blocks (Fig.5). Each volunteer was instructed to press a button as soon as a memory was recalled. Thus, in addition to fMRI data, behavioral data were also collected.

It is the first time that the impact of emojis on the autobiographical memory retrieval has been documented in fMRI. A significant impact of the sentimental content of the emojis was observed, both in the response time of the subjects and in the areas activated (with the use of the fMRI data). Furthermore it has been shown that this impact is significant even in the case of the use of a single word and not of a whole sentence, which biases the participant towards the sentimental content of the memory to be retrieved.

Specifically, it was observed that sentimentally incongruent emojis increase the reaction times and the number of omissions from the participants, while also activate brain regions related to the attention network and language processing, such as Broca's area, in agreement with previous studies. Furthermore, it has been shown that emojis convey non-verbal information that trigger brain areas related to face-emotion recognition such as the middle frontal gyrus, the left IPC and the (right) anterior fusiform gyrus; a finding that contrasts similar previous researches conducted with the use of emoticons instead of emojis [13]. The activation of the right fusiform gyrus is a significant finding. Due to the fact that emojis are actually drawings, and not facial representations by the sparse means of typographic symbols like emoticons, both the configural and featural mechanisms of the brain are able to process their image and hence, the face feature processing regions are activated.

Blind methods (such as ICA and BTD), which have only recently been proposed for task-related studies, have been also tested with similar findings to FSL. *Nevertheless, the area of posterior cingulate gyrus was only observed in the results of BTD, unlike FSL and GICA.* On the other hand, none of the blind methods tested were able to separate congruent from incongruent stimuli.

6 Fusion of EEG and fMRI via Soft Coupled Tensor Decompositions

Data fusion refers to the joint analysis of multiple datasets which provide complementary views of the same task. In this chapter of the thesis, the problem of jointly analyzing electroencephalography (EEG) and functional Magnetic Resonance Imaging (fMRI) data is considered. Analyzing both EEG and fMRI measurements is highly beneficial for studying brain function because these modalities have complementary spatiotemporal resolution: EEG offers good temporal resolution while fMRI offers good spatial resolution. Hence, the complementary nature of the spatiotemporal resolutions of EEG and FMRI motivates their fusion with the aim of achieving a better localization of the brain activity, both in time and space [14].

Different types of fusion can be realized. The earliest approaches for fusion of fMRI and EEG (and a large number of recent ones, are essentially "integrative" in nature. The rationale behind these methods is to employ objective functions for decomposition of the fMRI signal with constraints based on information obtained from EEG (or vice versa). Recently, the emphasis has been turned to "true" fusion, where the decomposition of the data from each modality can influence the other using all the common information that may exist. During optimization, the factors, which have been identified as common, are appropriately "coupled" and, thus, a bridge between the two modalities is established. Various ways to realize the coupling have been proposed depending on the coupled mode: a) coupling at the spatial domain with the use of the so-called lead-field matrix, which summarizes the volume conduction effects in the head b) coupling at the time domain using the convolution with an HRF, and c) coupling at the subjects domain, using the assumption that the same neural processes are reflected in both modalities with the same covariation. In all the aforementioned methods, the coupling between the corresponding modes is "hard", meaning that the shared factors are the same in the two datasets.

Although the multi-way nature of EEG has been exploited in earlier fusion methods, it has been neglected for fMRI. Furthermore, these methods rely on preprocessing of the fMRI data using the General Linear Model (GLM) framework. A spatial map of interest (areas of activation) per subject is extracted

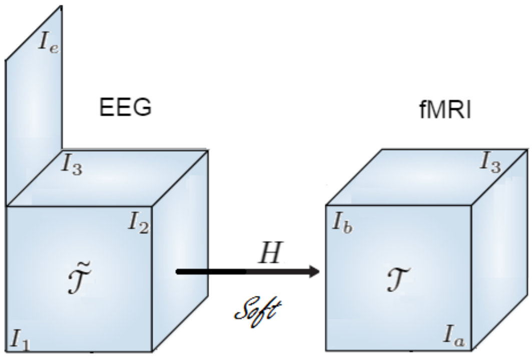

Figure 6: Schematic representation of the soft coupled CPDs at the time domain of EEG and fMRI.

from the fMRI data and all the spatial maps are stacked into a matrix (space $\times$ subjects), hence discarding the extra dimension of time and relying on Coupled Matrix Tensor Factorization (CMTF) to solve the joint BSS problem. In the GLM framework, a canonical HRF was assumed to be known (and invariant in space and among subjects), the expected signal changes are defined as regressors of interest in a multiple linear regression analysis and the estimated coefficients are tested against a null hypothesis. Intra- and inter-subject variability of HRF is known to exist, hence a possible misspecification of the HRF may lead to biased estimates of widespread activity in the brain. The use of the spatial maps of GLM categorizes such CMTF-based methods as "late" fusion or true fusion using multivariate features [3].

In this section of the thesis, we propose true "early" fusion of fMRI and EEG tensors via soft (assuming similarity and not strong-hard equality) coupling among modes. In our approach, we exploit the multi-way nature of both modalities and omit the GLM preprocessing step, in an effort to fully exploit the information underlying the raw data. We propose a framework for early fusion of fMRI and EEG using coupled CPD with "soft" coupling [15], which relies on similarity and not exact equality. Fusion based on raw data, although potentially quite challenging, may allow better inference. The coupling could be attempted in any of the modes, depending on the problem at hand. The schematic representation of the framework, proposed for coupling in the time domain, can be viewed at Fig. 6.

The CPDs of the 3rd-order fMRI tensor, $\boldsymbol{\mathcal{T}} \in \mathbb{R}^{I_a \times I_b \times I_3}$, and the 4th-order EEG tensor, $\tilde{\boldsymbol{\mathcal{T}}} \in \mathbb{R}^{I_e \times I_1 \times I_2 \times I_3}$, can be written as $\boldsymbol{T}_k \approx \boldsymbol{A}\boldsymbol{D}_k\boldsymbol{B}^\top$ and $\tilde{\boldsymbol{T}}_{k(1)} \approx \boldsymbol{E}\tilde{\boldsymbol{D}}_k(\tilde{\boldsymbol{B}} \odot \tilde{\boldsymbol{A}})^\top$, respectively, with $\tilde{\boldsymbol{T}}_{k(1)}$ being the mode-1 matricization of $\tilde{\boldsymbol{\mathcal{T}}}_k = \tilde{\boldsymbol{\mathcal{T}}}(:,:,:,k)$. $\boldsymbol{A} = \left[\boldsymbol{a}_1, \boldsymbol{a}_2, \ldots, \boldsymbol{a}_R\right]$ is a matrix that contains the weights of the R spatial components (I_a voxels), $\boldsymbol{B}, \boldsymbol{C}$ contain the associated time courses (I_b) and subject activation levels of fMRI (I_3), respectively, and $\boldsymbol{D}_k$ is the diagonal matrix formed from the kth row of $\boldsymbol{C}$. For the EEG case, matrices $\boldsymbol{E}, \tilde{\boldsymbol{A}}, \tilde{\boldsymbol{B}}, \tilde{\boldsymbol{C}}$ contain the weights of the associated ERPs (I_e), electrodes (I_1), trials amplitude (I_2) and the subject activation levels of EEG (I_3), respectively, and $\tilde{\boldsymbol{D}}_k$ is the diagonal matrix formed from the kth row of $\tilde{\boldsymbol{C}}$. The proposed cost function to minimize is given as:

$$\sum_{k=1}^{I_3} \|\boldsymbol{T}_k - \boldsymbol{A}\boldsymbol{D}_k\boldsymbol{B}^\top\|_F^2 + \sum_{k=1}^{I_3} \|\tilde{\boldsymbol{T}}_{k(1)} - \boldsymbol{E}\tilde{\boldsymbol{D}}_k(\tilde{\boldsymbol{B}} \odot \tilde{\boldsymbol{A}})^\top\|_F^2 + \lambda_B\|\boldsymbol{B}_{1:R_c} - \boldsymbol{H}\tilde{\boldsymbol{B}}_{1:R_c}\|_F^2, \tag{8}$$

with $\boldsymbol{L}$ being the lead-field matrix, used for the EEG forward problem, and $\boldsymbol{H}$ the matrix representing the convolution with the HRF and the down-sampling (due to the different sampling rate of the two modalities). R_c is the number of common components in the coupled mode(s), so there are $R - R_c$ and $\tilde{R} - R_c$ distinct components of fMRI and EEG, respectively.

The quadrilinear model of CPD that is selected for decomposing the EEG tensor assumes that every subject has exactly the same ERP, an assumption which is restrictive and can be overcome with the adoption of PARAFAC2, where $\boldsymbol{E}$ may vary with k. Thus, the CPD used for EEG can be replaced by PARAFAC2, with $\boldsymbol{E}_k = \boldsymbol{P}_k\boldsymbol{H}$ and $\boldsymbol{P}_k$ and $\boldsymbol{H}$, and the cost function is transformed to:

$$\sum_{k=1}^{I_3} \|\boldsymbol{X}_k - \boldsymbol{A}\boldsymbol{D}_k\boldsymbol{B}^\top\|_F^2 + \sum_{k=1}^{I_3} \|\boldsymbol{P}_k^\top\tilde{\boldsymbol{T}}_{k(1)} - \boldsymbol{H}\tilde{\boldsymbol{D}}_k(\tilde{\boldsymbol{B}} \odot \tilde{\boldsymbol{A}})^\top\|_F^2 + \lambda_B\|\boldsymbol{B}_{1:R_c} - \boldsymbol{H}\tilde{\boldsymbol{B}}_{1:R_c}\|_F^2. \tag{9}$$

We demonstrate, with simulated data, the advantage of the proposed method over methods based on Independent Component Analysis (ICA), hard coupling and uncoupled CPD per modality. This is an attempt to benefit from the multi-way nature of *both* modalities, following an "early true" fusion (hence bypassing the need to rely on features). Performance gains have been reported compared to ICA methods as well as to the separate analyses of the datasets. The use of coupled PARAFAC2-CPD was seen to outperform the coupled CPD in the presence of shifts in the ERPs per subject. A simple mean-ERP analysis prior to the joint analysis could provide an indication of the amount of the shift in the ERPs, in order to select which of the soft coupled tensor decompositions shall be used. Future work will include studies with real data, comparisons with methods based on Independent Vector Analysis (IVA) and alternative tensor models (e.g., Block Term Decomposition). Moreover, a more systematic selection of the λ values will be sought for.

References

[1] M. A. Lindquist, "The statistical analysis of fMRI data," *Statistical Science*, vol. 23, no. 4, pp. 439–464, Jun. 2008.

[2] S. Theodoridis, *Machine Learning: A Bayesian and Optimization Perspective.* Academic Press, 2015.

[3] D. Lahat, T. Adalı, and C. Jutten, "Multimodal data fusion: An overview of methods, challenges, and prospects," *Proc. IEEE*, no. 9, Sep. 2015.

[4] L. De Lathauwer, "Decompositions of a higher-order tensor in block terms–Part I: Lemmas for partitioned matrices," *SIAM J. Matrix Anal. Appl.*, vol. 30, no. 3, pp. 1022–1032, Sep. 2008.

[5] A. H. Andersen and W. S. Rayens, "Structure-seeking multilinear methods for the analysis of fMRI data," *NeuroImage*, no. 2, pp. 728–739, Jun. 2004.

[6] V. D. Calhoun and T. Adalı, "A review of group ICA for fMRI data and ICA for joint inference of imaging, genetic, and ERP data," *NeuroImage*, vol. 45, no. 1, pp. 163–172, Mar. 2009.

[7] M. Morante, Y. Kopsins, and S. Theodoridis, "Information assisted dictionary learning for fMRI data analysis," arXiv:1802.01334v1, Feb. 2018.

[8] A. Stegeman, "Comparing Independent Component Analysis and the PARAFAC model for artificial multi-subject fMRI data," Unpublished Technical Report, Univ. of Groeningen, Feb. 2007.

[9] N. E. Helwig and S. Hong, "A critique of Tensor Probabilistic Independent Component Analysis: implications and recommendations for multi-subject fMRI data analysis," *J. Neuroscience Methods*, no. 2, pp. 263–273, Mar. 2013.

[10] C. F. Beckmann and S. M. Smith, "Tensorial extensions of independent component analysis for multisubject fMRI analysis," *NeuroImage*, no. 1, pp. 294–311, Mar. 2005.

[11] A. H. Phan, P. Tichavský, and A. Cichocki, "CANDECOMP/PARAFAC decomposition of high-order tensors through tensor reshaping," *IEEE Trans. Signal Process.*, no. 19, pp. 4847–4860, Oct. 2013.

[12] R. A. Harshman, "PARAFAC2: Mathematical and technical notes," *UCLA Working Papers in Phonetics*, pp. 30–44, 1972.

[13] M. Yuasa, K. Saito, and N. Mukawa, "Brain activity when reading sentences and emoticons: An fMRI study of verbal and nonverbal communication," *Electr. and Commun. in Japan*, no. 5, pp. 1797–1803, Jan. 2011.

[14] E. Karahan, P. A. Rojas-Lopés, M. L. Bringas-Vega, P. A. Valdés-Hernandéz, and P. A. Valdes-Sosa, "Tensor analysis and fusion of multimodal brain images," *Proc. IEEE*, vol. 103, Sep. 2015.

[15] N. Seichepine, S. Essid, C. Fevotte, and O. Cappe, "Soft nonnegative matrix co-factorization," *IEEE Trans. Signal Process.*, no. 22, Nov. 2014.